Supplementary Data

Supplementary Table 1. Composition of training and testing sets for each treatment cohort, including number of patients with available post-treatment response and survival information. pCR, pathologic complete response, MPR, major pathologic response, RECIST, Response Evaluation Criteria In Solid Tumors, RFS, recurrence-free survival, PFS, progression-free survival.

	Training					Testing				
		Response		Prognosis			Response		Prognosis	
Cohort	*Notation*	n	Endpoint	n	Endpoint	*Notation*	n	Endpoint	n	Endpoint
BRCA-ACT	D_{tr}^1	98	pCR	63	RFS	D_{te}^1	144	pCR	94	RFS
BRCA-TCHP	D_{tr}^2	69	pCR	0	-	D_{te}^2	60	pCR	0	-
NSCLC-PLAT	D_{tr}^3	53	RECIST response	53	PFS	D_{te}^3	44	RECIST response	39	PFS
NSCLC-TRI	D_{tr}^4	44	MPR	44	RFS	D_{te}^4	46	MPR	46	RFS

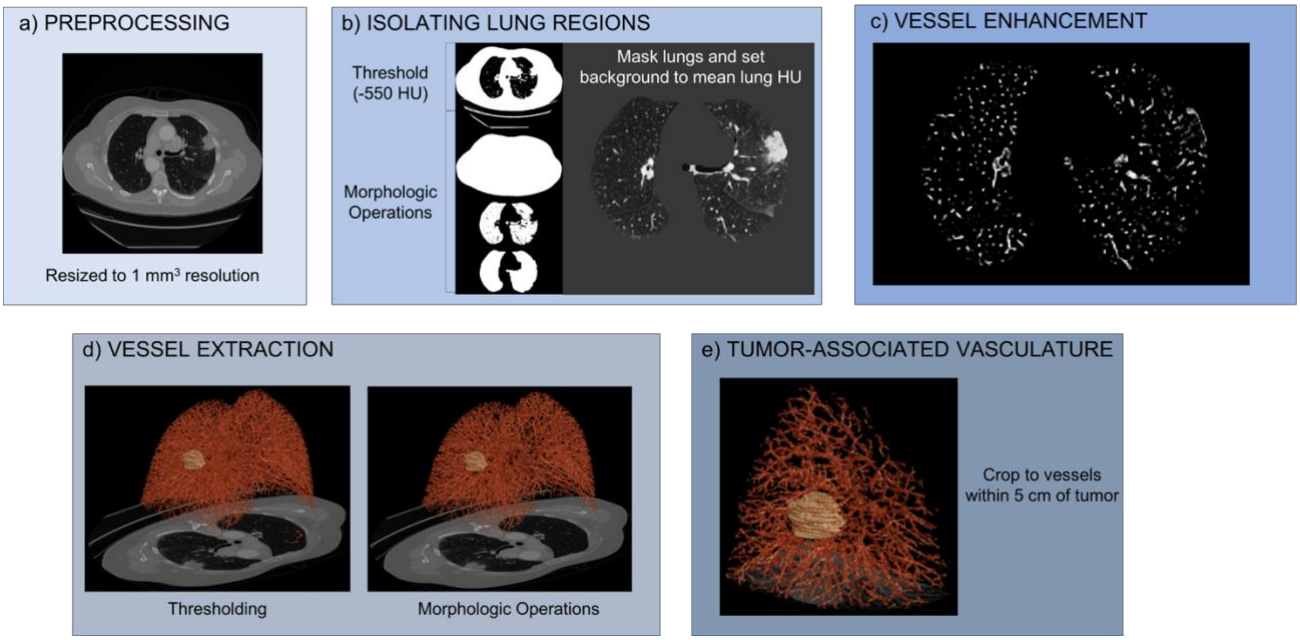

Supplementary Figure 1. a) all volumes were resized to consistent isotropic resolution, b) a mask of the lung was obtained one slice at a time to isolate the lungs within a CT volume. First, a threshold of -550 HU was applied to identify non-lung, body tissue (mask 1). Hole filling and largest object detection were performed to obtain a mask of the full body (mask 2). The difference between mask 2 and 1 giving a raw lung segmentation (mask 3). Mask 3 was refined by morphologic operations such as opening, closing, and hole filling, to yield a final lung tissue mask. The average attenuation value within the lungs was computed and used to fill voxels corresponding to non-lung tissue so as not to create edges with shape attenuation changes at the lung interface. c) a vessel enhancement filter was applied to the lung volume to identify bright objects with tubular, vessel-like shapes (see Supplementary Implementation Details). d) Thresholding via Otsu's method was applied to the vessel-enhanced volume to isolate vessels from background (left). Morphologic processing, such as the removal of small and spherical objects, was applied to refine the vessel skeleton and remove noise (right). e) Finally, the volume is cropped to the tumor and its surrounding vasculature out to 5 cm in all directions.

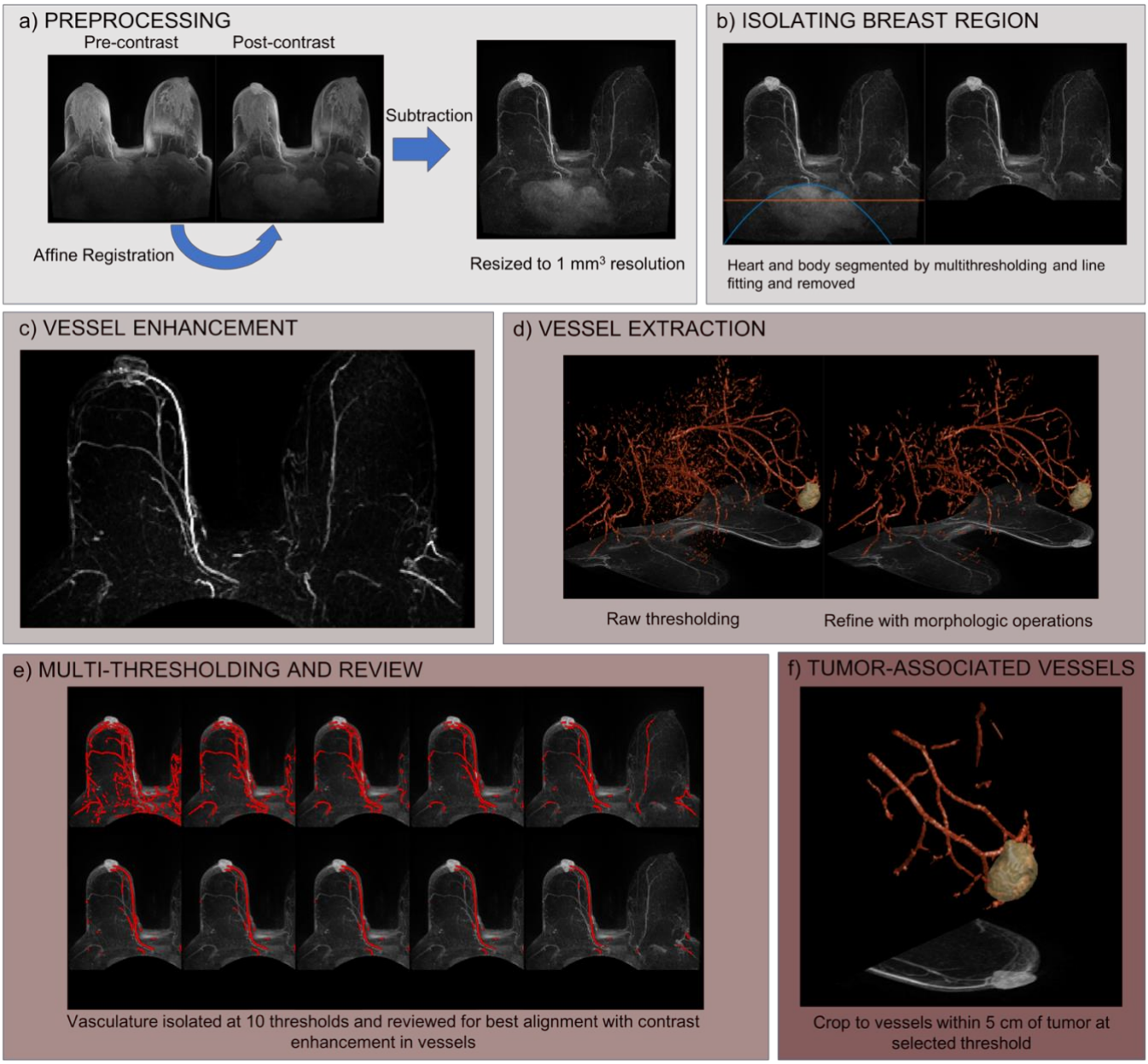

Supplementary Figure 2. a) An affine registration was performed to align the pre-contrast and first post-contrast DCE-MRI acquisitions, and the difference in image intensities was computed to yield subtraction volumes. Tissues perfused with contrast agent (such as the vessels and tumor) appear brightest, while much of the signal from surrounding breast tissue is removed. b) The heart was identified by multi-thresholding and largest object detection. Lines were fit to its upper edge (blue) and centroid (orange) and used to mask out contrast enhancement outside the breasts. c) a vessel enhancement filter was applied to the image with settings scaled relative to the magnitude of scan intensity (see Supplementary implementation details. d) Once a threshold was applied to isolate vessel voxels from background, the same morphologic operations applied in Supplementary Figure 1d were applied to remove artifacts. e) Thresholding was applied using Otsu's method at ten different thresholds, each yielding an increasingly sparse vessel segmentation. Due to the non-quantitative nature of MRI, the optimal threshold differed between scans and was determined through outcome-blinded manual review. f) Finally, volumes were cropped to the local tumor vasculature at a distance of 5 cm from the tumor in all directions.

Supplementary Table 2. Full list of 61 QuanTAV Morphology features extracted.

Features	Description
Statistics of torsion per branch (f1-f5)	*Mean*, standard deviation (*std*), maximum (*max*), skewness (*skew*), and kurtosis (*kurt*) of torsion across all branches
Statistics of curvature standard deviation per branch (f6-f10)	*Mean, std, max, skew, kurt* of the standard deviation of curvature measured along each branch
Statistics of mean curvature per branch (f11-f15)	*Mean, std, max, skew, kurt* of the average curvature measured along each branch
Statistics of maximum curvature per branch (f16-f20)	*Mean, std, max, skew, kurt* of the maximum curvature measured along each branch
Statistics of curvature skewness per branch (f21-f25)	*Mean, std, max, skew, kurt* of the skewness of curvature measured along each branch
Statistics of curvature kurtosis per branch (f26-f30)	*Mean, std, max, skew, kurt* of the kurtosis of curvature measured along each branch
Statistics of global vascular curvature (f31-f35)	*Mean, std, max, skew, kurt* of the curvature measured across all branches combined
Histogram of global vascular curvature (f36-f45)	10-bin histogram of the curvature measured across all points of the vessel volume
Histogram of torsion (f46-f55)	10-bin histogram of the torsion measured across all branches combined
Total vessel volume (f56-f58)	Vessel volume (f56), vessel volume normalized to the total size of the 3D region of interest (f57), vessel volume normalized to the volume of the tumor (f58).
Total vessel length (f59)	Total length of vessels within the region of interest
Tumor feeding branches (f60, f61)	Number (f60) and percentage (f61) of vessel branches that enter the tumor volume from the surrounding tumor environment.

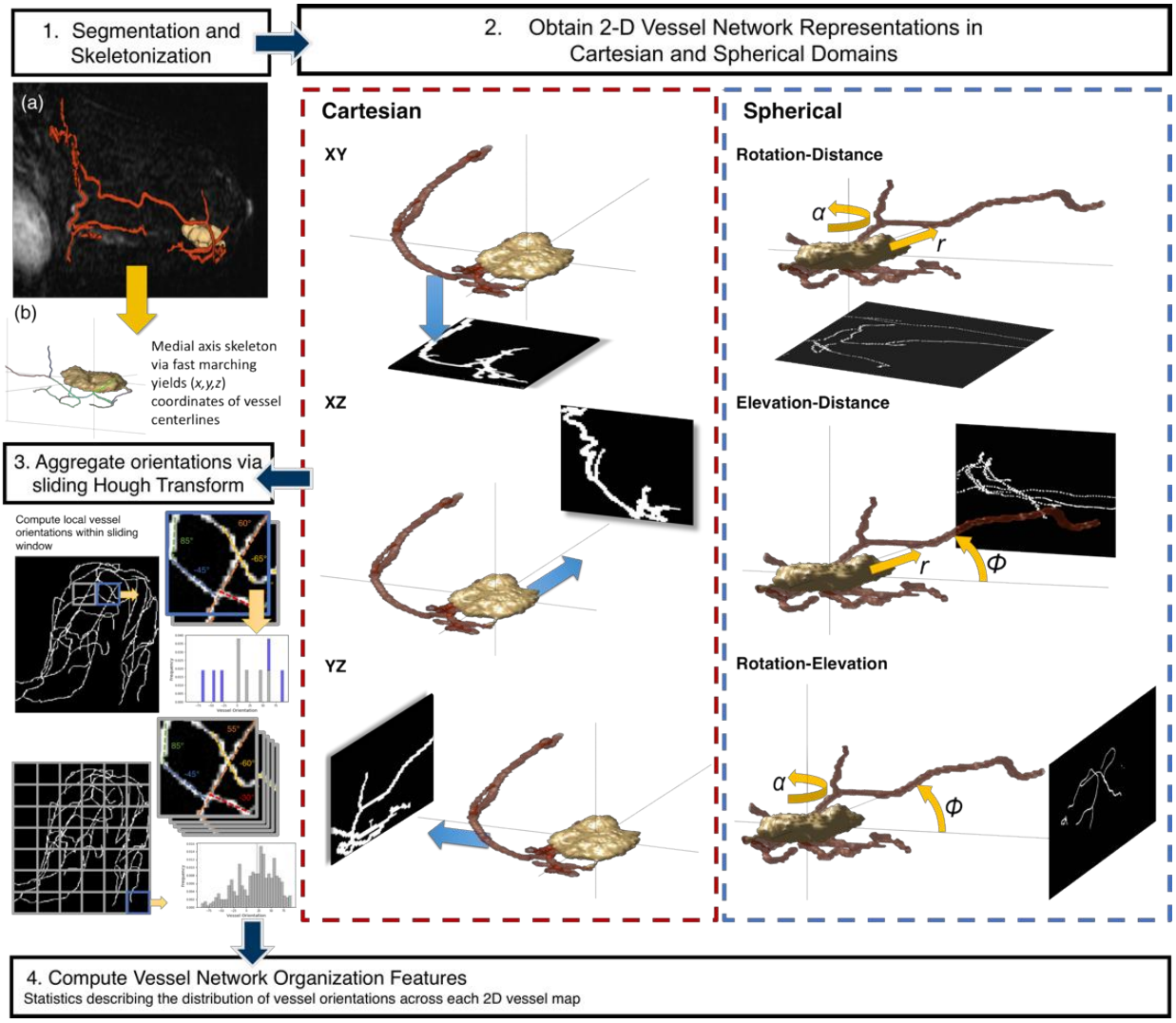

Supplementary Figure 3. Workflow for computing features describing tumor-associated vasculature organization. QuanTAV Spatial Organization[29] features quantify the distribution of local vessels within a fixed radius surrounding the tumor by creating 2D projection images of a vessel's position in cartesian (X.Y,Z) space and spherical (rotation and elevation relative to the tumor surface, and distance relative to the tumor surface). Each project image is then analyzed locally within a sliding window. The Hough transform[93] is applied to detect lines within the window and quantify their orientation. The most prominent vessel orientations, up to a maximum of five, are stored. Statistics of the distribution of vessel orientations form the set of QuanTAV spatial organization features. The maximum distance from the tumor and size of the sliding window are optimized for each cancer domain/imaging modality by performance of a classifier in cross-validation in the training sets.

Supplementary Table 3. Full list of 30 QuanTAV Spatial Organization features extracted.

Features	Description
Statistics of vessel orientation along XY projection image (f1-f5)	*Mean*, *median* (med), standard deviation (*std*), skewness (*skew*), and kurtosis (*kurt*) of local vessel orientations computed across XY vessel map
Statistics of vessel orientation along the XZ projection image (f6-f10)	*Mean*, *med, std, skew, kurt* of local vessel orientations computed across XZ vessel map
Statistics of vessel orientation along the YZ projection image (f11-f15)	*Mean, std, max, skew, kurt* of local vessel orientations computed across XZ vessel map
Statistics of vessel orientation along the rotation-elevation projection image (f16-f20)	*Mean, std, max, skew, kurt* of local vessel orientations computed across vessel map of rotation and elevation with respect to the tumor
Statistics of vessel orientation along the distance-rotation projection image (21-f25)	*Mean, std, max, skew, kurt* of local vessel orientations computed across vessel map of distance and rotation with respect to the tumor
Statistics of vessel orientation along the distance-elevation projection image (f26-f30)	*Mean, std, max, skew, kurt* of local vessel orientations computed across vessel map of distance and elevation with respect to the tumor

Supplementary Table 4. Top features and corresponding coefficients for LDA classifier to predict pathologic response in HER2-negative breast cancer patients receiving BRCA-ACT. Expression of features with positive coefficients contributes to a response prediction, while expression of features with negative coefficients contributes to a prediction of non-response.

Feature Name	Coefficient
QuanTAV Spatial Organization - YZ - Skewness	0.18
QuanTAV Spatial Organization - Distance-Elevation - Median	0.72
QuanTAV Spatial Organization - Distance-Elevation - Mean	-0.16
QuanTAV Spatial Organization - XZ - Skewness	0.060
QuanTAV Spatial Organization - YZ - Median	0.88
QuanTAV - Torsion - Mean	-0.44
Constant	-0.23

Supplementary Table 5. Area under the receiver operating characteristic curve (AUC) of QuanTAV response score models and significance.

	Training	Testing	
Cohort	*AUC (95% CI)*	*AUC (95% CI)*	*p-value*
BRCA-ACT	0.63 (0.55-0.70)	0.65 (0.54-0.76)	0.009
BRCA-TCHP	0.65 (0.58-0.72)	0.63 (0.47-0.76)	0.042
NSCLC-PLAT	0.68 (0.56-0.79)	0.70 (0.54-0.85)	0.024
NSCLC-TRI	0.71 (0.60-0.81)	0.71 (0.51-0.84)	0.0093

Supplementary Table 6. Univariate (UVA) and multivariable (MVA) analysis of QuanTAV response score and available clinical variables for prediction of pathologic response to BRCA-ACT. Clinical variables that were individually significant in the training set (hormone receptor status) were incorporated into logistic regression models alone and with QuanTAV response score, and evaluated on the testing set. OR, odds ratio; p, p-value.

	Training set		**(n=98)**		**Testing set**		**(n=144)**	
	Univariable		*Multivariable*		*Univariable*		*Multivariable*	
Variable	Odds Ratio (95% CI)	p	Odds Ratio (95% CI)	p	Odds Ratio (95% CI)	p	Odds Ratio (95% CI)	p
QuanTAV Response Score	0.09 (0.01 - 0.90)	**0.046**	0.05 (0.00 - 0.87)	**0.040**	0.07 (0.01 - 0.63)	**0.018**	0.02 (0.00 - 0.32)	**0.005**
Hormone Receptor Status (Positive vs. Negative)	4.73 (1.77 - 12.65)	**0.002**	5.99 (2.01 - 17.79)	**0.001**	5.10 (2.02 - 12.90)	**0.001**	7.24 (2.49 - 21.05)	**<1E-5**
Age (per year increase)	1.02 (0.97 - 1.07)	0.495	1.06 (0.99 - 1.12)	0.072	1.06 (1.01 - 1.11)	**0.012**	1.06 (1.01 - 1.12)	**0.019**
Lesion Diameter (per mm increase)	1.17 (0.96 - 1.41)	0.115	1.23 (0.98 - 1.53)	0.069	1.09 (0.93 - 1.28)	0.268	1.05 (0.88 - 1.26)	0.559

Supplementary Table 7. The set of features selected by the elastic-net Cox regression model as being most prognostic of RFS from initiation of neoadjuvant chemotherapy among breast cancer patients receiving BRCA-ACT and their corresponding hazard ratios. The hazard ratios shown here reflect the risk associated with an increase of one standard deviation in feature value on the training set. A hazard ratio of less than 1 implies that an increase in that feature's value is associated with reduced risk, while a hazard ratio greater than 1 implies the opposite.

Feature Name	**Hazard Ratio**
QuanTAV Spatial Organization - Distance-Rotation - Skewness	0.89
QuanTAV Spatial Organization - Distance-Elevation - Standard Deviation	0.89
QuanTAV Spatial Organization - Rotation-Elevation - Skewness	0.90
QuanTAV Spatial Organization - Distance-Rotation - Standard Deviation	0.93
QuanTAV Spatial Organization - XZ - Kurtosis	0.93
Ratio of Vessel to Tumor Volume	0.96
QuanTAV Morphology - Torsion Histogram - Bin 2	0.98
QuanTAV Spatial Organization - YZ - Skewness	1.00
QuanTAV Spatial Organization - YZ - Kurtosis	1.03
QuanTAV Morphology - Torsion - Mean	1.03
No. Vessels Feeding Tumor	1.05
QuanTAV Morphology - Torsion - Standard Deviation	1.06
QuanTAV Spatial Organization - Rotation-Elevation - Kurtosis	1.08
Percentage of Vessels Feeding Tumor	1.11

Supplementary Table 8. Hazard ratio (HR), concordance index (C-index), and p-value of the HR for each prognostic model in the training and testing sets.

		Training			**Testing**		
Cohort	**Signature**	*Hazard Ratio (95% CI)*	*C-index*	*p*	*Hazard Ratio (95% CI)*	*C-index*	*p*
BRCA-ACT	*Risk Score*	1.43 (1.24-1.66)	0.79	**<1e-5**	1.25 (1.08-1.44)	0.66	**0.002**
	Risk Group	10.75 (1.43-80.61)	0.66	**0.021**	4.25 (1.29-14.07)	0.62	**0.018**
NSCLC-PLAT	*Risk Score*	1.32 (1.16-1.50)	0.77	**1.6e-5**	1.12 (0.96-1.31)	0.61	0.14
	Risk Group	7.19 (2.85-18.14)	0.71	**3.0e-5**	2.29 (1.07-4.94)	0.62	**0.034**
NSCLC-TRI	*Risk Score*	1.32 (1.16-1.50)	0.81	**1.9e-5**	1.28 (1.01-1.62)	0.66	**0.039**
	Risk Group	20.33 (2.68-154.12)	0.74	**4.5e-5**	3.77 (1.09-13.00)	0.64	**0.036**

Supplementary Table 9. Cox proportional hazard univariable (UVA) and multivariable (MVA) analysis of recurrence free survival following BRCA-ACT treatment, including QuanTAV risk score, QuanTAV risk groups, baseline clinical variables, and post-chemotherapy response.

	Univariable		**Multivariable** Risk Score (Continuous)		**Multivariable** Risk Groups (Categorical)	
Variable	Hazard Ratio (95% CI)	p	Hazard Ratio (95% CI)	p	Hazard Ratio (95% CI)	p
QuanTAV Risk Score (increase of 1)	1.25 (1.08 - 1.44)	**0.002**	1.20 (1.04 - 1.40)	**0.014**	--	--
QuanTAV Risk Group (High vs. Low Risk)	4.25 (1.29 - 14.07)	**0.018**	--	--	5.51 (1.41 - 21.49)	**0.014**
Hormone receptor status (positive vs. negative)	0.45 (0.22 - 0.95)	**0.036**	0.40 (0.18 - 0.89)	**0.025**	0.36 (0.16 - 0.81)	**0.014**
Age (per year increase)	0.95 (0.92 - 0.99)	**0.017**	0.94 (0.90 - 0.99)	**0.013**	0.94 (0.90 - 0.98)	**0.007**
Largest lesion diameter (per mm increase)	1.10 (1.00 - 1.22)	0.062	1.01 (0.90 - 1.14)	0.821	1.02 (0.90 - 1.15)	0.746
Functional Tumor Volume (per 10cc increase)	1.21 (1.07 - 1.36)	**0.002**	1.13 (1.01 - 1.28)	**0.040**	1.16 (1.04 - 1.31)	**0.011**

Supplementary Table 10. Correlation of features in BRCA-ACT risk score associated with functional tumor volume (FTV) on DCE-MRI.

Feature Name	Correlation Coefficient	P-value
QuanTAV Spatial Organization - XZ - Kurtosis	0.0253	0.8086
QuanTAV Spatial Organization - YZ - Skewness	-0.0392	0.7074
QuanTAV Spatial Organization - YZ - Kurtosis	-0.1246	0.2315
QuanTAV Spatial Organization - Rotation-Elevation - Skewness	0.0006	0.9954
QuanTAV Spatial Organization - Rotation-Elevation - Kurtosis	-0.1103	0.2900
QuanTAV Spatial Organization - Distance-Rotation - Standard Deviation	-0.0843	0.4192
QuanTAV Spatial Organization - Distance-Rotation - Skewness	-0.2126	**0.0396**
QuanTAV Spatial Organization - Distance-Elevation - Standard Deviation	-0.2115	**0.0407**
QuanTAV Morphology - Torsion - Mean	0.0946	0.3645
QuanTAV Morphology - Torsion - Standard Deviation	0.1237	0.2348
Ratio of Vessel to Tumor Volume	-0.1905	0.0660
QuanTAV Morphology - Torsion Histogram - Bin 2	-0.1549	0.1361
No. Vessels Feeding Tumor	0.2294	**0.0262**
Percentage of Vessels Feeding Tumor	0.5515	**<1E-5**

Supplementary Table 11. Top features and corresponding coefficients for LDA classifier to predict pathologic response in HER2-positive breast cancer patients receiving HER2-targeted neoadjuvant chemotherapy (BRCA-TCHP). Expression of features with positive coefficients contributes to a response prediction, while expression of features with negative coefficients contributes to a prediction of non-response.

Feature Name	Coefficient
QuanTAV Spatial Organization - XY - Skewness	-0.52
QuanTAV Spatial Organization - Distance-Elevation - Mean	0.30
QuanTAV Spatial Organization - Distance-Elevation - Median	0.48
QuanTAV Morphology - Torsion Histogram - Bin 7	-0.50
Constant	0.029

Supplementary Table 12. Univariate (UVA) and multivariable (MVA) analysis of QuanTAV response score and available clinical variables for prediction of pathologic response to BRCA-TCHP. Clinical variables that were individually significant in the training set (hormone receptor status) were incorporated into logistic regression models alone and with QuanTAV response score, and evaluated on the testing set. OR, odds ratio; p, p-value.

	Training set		**(n=69)**		**Testing set**		**(n=60)**	
	Univariable		*Multivariable*		*Univariable*		*Multivariable*	
Variable	Odds Ratio (95% CI)	p	Odds Ratio (95% CI)	p	Odds Ratio (95% CI)	p	Odds Ratio (95% CI)	p
QuanTAV Response Score	0.06 (0.00 - 0.69)	**0.024**	0.13 (0.01 - 1.88)	0.135	0.17 (0.01 - 1.88)	0.148	0.17 (0.01 - 2.38)	0.188
Hormone receptor status (positive vs. negative)	3.68 (1.23 - 11.05)	**0.020**	3.11 (0.91 - 10.68)	0.072	3.89 (1.23 - 12.29)	**0.021**	3.86 (1.17 - 12.77)	**0.027**
Age (per year increase)	1.02 (0.97 - 1.06)	0.475	1.02 (0.98 - 1.07)	0.343	0.99 (0.94 - 1.04)	0.739	1.00 (0.95 - 1.06)	0.865
Largest lesion diameter (per mm increase)	1.03 (0.89 - 1.19)	0.730	1.01 (0.85 - 1.20)	0.925	1.00 (0.82 - 1.23)	0.993	0.99 (0.77 - 1.27)	0.934
Clinical Stage (per stage increase)	1.01 (0.46 - 2.18)	0.986	0.74 (0.29 - 1.88)	0.533	0.97 (0.33 - 2.83)	0.956	1.03 (0.27 - 3.92)	0.964

Supplementary Table 13. Top features and corresponding coefficients for LDA classifier to predict RECIST response in NSCLC patients receiving platinum-based neoadjuvant chemotherapy (NSCLC-PLAT). Expression of features with positive coefficients contributes to a response prediction, while expression of features with negative coefficients contributes to a prediction of non-response.

Feature Name	**Coefficient**
QuanTAV Spatial Organization - XZ - Kurtosis	0.86
QuanTAV Spatial Organization - XZ - Skewness	-0.53
QuanTAV Spatial Organization - Distance-Rotation - Skewness	-0.44
QuanTAV Spatial Organization - Distance-Elevation - Standard Deviation	-0.98
QuanTAV Spatial Organization - XZ - Median	-1.02
QuanTAV Spatial Organization - Distance-Rotation - Mean	-0.22
Constant	-0.015

Supplementary Table 14. Univariate (UVA) and multivariable (MVA) analysis of QuanTAV response score and available clinical variables for prediction of RECIST response in NSCLC-PLAT recipients. Clinical variables that were individually significant in the training set (age) were incorporated into logistic regression models alone and with QuanTAV response score, and evaluated on the testing set. OR, odds ratio; p, p-value.

	Training set		**(n=53)**		**Testing set**		**(n=44)**	
	Univariable		*Multivariable*		*Univariable*		*Multivariable*	
Variable	Odds Ratio (95% CI)	p	Odds Ratio (95% CI)	p	Odds Ratio (95% CI)	p	Odds Ratio (95% CI)	p
QuanTAV Response Score	0.04 (0.00 - 0.45)	**0.010**	0.03 (0.00 - 0.55)	**0.017**	0.04 (0.00 - 0.62)	**0.021**	0.03 (0.00 - 0.93)	**0.045**
Age (per year increase)	0.94 (0.89 - 1.00)	**0.048**	0.95 (0.89 - 1.03)	0.228	1.03 (0.98 - 1.07)	0.232	1.03 (0.98 - 1.09)	0.236
Sex (male vs. female)	0.37 (0.12 - 1.12)	0.078	0.35 (0.09 - 1.42)	0.141	0.93 (0.27 - 3.17)	0.902	0.87 (0.20 - 3.79)	0.856
Stage (per stage increase)	1.02 (0.50 - 2.10)	0.950	1.05 (0.38 - 2.91)	0.924	1.44 (0.55 - 3.78)	0.458	1.06 (0.30 - 3.72)	0.925
Longest diameter (per mm increase)	0.99 (0.97 - 1.01)	0.534	0.99 (0.96 - 1.03)	0.641	1.01 (0.99 - 1.02)	0.454	1.00 (0.98 - 1.03)	0.670
Histology (SCC/other vs. Adenocarcinoma)	0.24 (0.04 - 1.28)	0.094	0.25 (0.03 - 2.24)	0.213	1.02 (0.29 - 3.65)	0.975	1.97 (0.40 - 9.62)	0.404
Former smoker (Yes vs. No)	3.75 (0.68 - 20.63)	0.129	7.11 (0.61 - 82.78)	0.118	0.40 (0.07 - 2.35)	0.311	0.29 (0.04 - 2.16)	0.226

Supplementary Table 15. The set of features selected by the elastic-net Cox regression model as being most prognostic of PFS following inception of platinum-based chemotherapy (NSCLC-PLAT) among lung cancer patients and corresponding hazard ratios in the training set. The hazard ratios shown here reflect the risk of an increase of one standard deviation in feature value on the training set. A hazard ratio of less than 1 implies that an increase in that feature's value is associated with reduced risk, while a hazard ratio greater than 1 implies the opposite.

Feature Name	**Hazard Ratio**
Normalized Vessel Volume	0.48
QuanTAV Morphology - Global Curvature - Kurtosis	0.61
QuanTAV Spatial Organization - XZ - Skewness	0.73
QuanTAV Morphology - Kurtosis of Curvature Per Vessel - Standard Deviation	0.75
QuanTAV Morphology - Global Curvature - Skewness	0.86
QuanTAV Morphology - Maximum Curvature per Vessel - Mean	0.88
QuanTAV Morphology - Skewness of Curvature Per Vessel - Kurtosis	0.90
QuanTAV Morphology - Skewness of Curvature Per Vessel - Skewness	0.97
QuanTAV Morphology - Torsion Histogram - Bin 8	1.07
QuanTAV Spatial Organization - Distance-Elevation - Mean	1.16
QuanTAV Spatial Organization - Distance-Rotation - Kurtosis	1.28
QuanTAV Spatial Organization - Distance-Elevation - Standard Deviation	1.80
QuanTAV Spatial Organization - Distance-Rotation - Standard Deviation	2.24
QuanTAV Spatial Organization - XZ - Median	2.70
QuanTAV Spatial Organization - Distance-Elevation - Kurtosis	2.86

Supplementary Table 16. Cox proportional hazard univariable (UVA) and multivariable (MVA) analysis of 10-year progression free survival following NSCLC-PLAT treatment, including QuanTAV risk score, QuanTAV risk groups, baseline clinical variables, and post-chemotherapy response.

	Univariable		**Multivariable** Risk Score (Continuous)		**Multivariable** Risk Groups (Categorical)	
Variable	Hazard Ratio (95% CI)	p	Hazard Ratio (95% CI)	p	Hazard Ratio (95% CI)	p
QuanTAV Risk Score (increase of 1)	1.12 (0.96 - 1.31)	0.141	1.10 (0.93 - 1.31)	0.260	--	--
QuanTAV Risk Group (High vs. Low Risk)	2.29 (1.07 - 4.94)	**0.034**	--	--	2.53 (1.10 - 5.80)	**0.028**
Age (per year increase)	0.99 (0.96 - 1.02)	0.657	1.00 (0.97 - 1.03)	0.830	1.00 (0.97 - 1.03)	0.934
Sex (male vs. female)	1.06 (0.52 - 2.18)	0.868	1.28 (0.56 - 2.96)	0.560	1.43 (0.63 - 3.27)	0.389
Stage (per stage increase)	1.43 (0.79 – 2.58)	0.241	1.41 (0.68 – 2.93)	0.360	1.60 (0.72 – 3.54)	0.248
Longest diameter (per mm increase)	1.00 (0.99 - 1.01)	0.543	1.00 (0.99 - 1.01)	0.692	1.00 (0.99 - 1.02)	0.436
Histology (Adenocarcinoma vs. SCC/other)	0.82 (0.38 - 1.77)	0.619	0.92 (0.42 - 2.01)	0.827	0.91 (0.42 - 1.97)	0.807
Former smoker	0.70 (0.30 - 1.65)	0.419	0.72 (0.29 - 1.80)	0.477	0.76 (0.30 - 1.91)	0.565

Supplementary Table 17. Top features and corresponding coefficients for LDA classifier to predict pathologic response in NSCLC patients receiving neoadjuvant chemoradiation (NSCLC-TRI). Expression of features with positive coefficients contributes to a response prediction, while expression of features with negative coefficients contributes to a prediction of non-response.

Feature Name	**Coefficient**
QuanTAV Spatial Organization - Distance-Elevation - Kurtosis	-0.89
QuanTAV Morphology - Skewness of Curvature Per Vessel - Kurtosis	1.21
QuanTAV Spatial Organization - Distance-Rotation - Mean	0.71
QuanTAV Morphology - Torsion - Max	0.41
Constant	-0.14

Supplementary Table 18. Univariate (UVA) and multivariable (MVA) analysis of QuanTAV response score and available clinical variables for prediction of pathologic response in NSCLC-TRI recipients. Clinical variables that were individually significant in the training set (histology) were incorporated into logistic regression models alone and with QuanTAV response score, and evaluated on the testing set. OR, odds ratio; p, p-value.

	Training set		**(n=44)**		**Testing set**		**(n=46)**	
	Univariable		*Multivariable*		*Univariable*		*Multivariable*	
Variable	Odds Ratio (95% CI)	p	Odds Ratio (95% CI)	p	Odds Ratio (95% CI)	p	Odds Ratio (95% CI)	p
QuanTAV Response Score	0.02 (0.00-0.25)	**0.003**	0.00 (0.00-0.25)	**0.017**	0.06 (0.00-0.64)	**0.020**	0.00 (0.00-0.78)	**0.042**
Age (per year increase)	1.00 (0.94-1.07)	0.911	1.04 (0.92-1.19)	0.510	1.03 (0.98-1.09)	0.283	0.95 (0.84-1.06)	0.338
Sex (male vs. female)	3.25 (0.93-11.41)	0.066	21.48 (0.68-675.21)	0.081	2.00 (0.59-6.83)	0.269	1.04 (0.11-9.94)	0.972
Stage (IIIA vs IIIB)	N/A	N/A	N/A	N/A	0.13 (0.01-1.27)	0.080	0.15 (0.01-3.51)	0.238
Longest diameter (per mm increase)	0.99 (0.97-1.01)	0.160	0.97 (0.90-1.04)	0.407	0.95 (0.92-0.98)	**0.004**	0.97 (0.93-1.02)	0.208
Histology (Adenocarcinoma vs. SCC/other)	8.36 (1.52-46.15)	**0.015**	35.61 (1.37-928.63)	**0.032**	9.43 (2.28-39.04)	**0.002**	15.47 (1.40-171.31)	**0.026**
ECOG performance status (per grade increase)	3.06 (0.74-12.65)	0.122	7.45 (0.40-137.06)	0.177	1.00 (0.24-4.20)	1.000	0.41 (0.02-10.16)	0.583
Chemotherapy (Carboplatin vs. Cisplatin)	1.53 (0.37-6.35)	0.557	5.44 (0.15-193.86)	0.353	0.19 (0.05-0.78)	**0.021**	0.11 (0.00-3.33)	0.205
Radiotherapy Induction Dose (per Gy increase)	0.98 (0.92-1.04)	0.560	1.00 (0.89-1.12)	0.960	0.95 (0.89-1.01)	0.123	0.90 (0.78-1.04)	0.140

Supplementary Table 19. The set of features selected by the elastic-net Cox regression model as being most prognostic of RFS from date of surgery among lung cancer patients receiving trimodality therapy and corresponding hazard ratios in the training set. The hazard ratios shown here reflect the risk of an increase of one standard deviation in feature value on the training set. A hazard ratio of less than 1 implies that an increase in that feature's value is associated with reduced risk, while a hazard ratio greater than 1 implies the opposite.

Feature Name	**Hazard Ratio**
QuanTAV Morphology - Skewness of Curvature Per Vessel - Kurtosis	0.71
QuanTAV Spatial Organization - YZ - Skewness	0.77
QuanTAV Morphology - Torsion Histogram - Bin 9	0.82
QuanTAV Spatial Organization - Distance-Rotation - Median	0.90
QuanTAV Spatial Organization - XY - Standard Deviation	0.92
QuanTAV Spatial Organization - Rotation-Elevation - Skewness	0.93
QuanTAV Spatial Organization - YZ - Kurtosis	0.98
QuanTAV Morphology - Torsion Histogram - Bin 10	0.99
QuanTAV Spatial Organization - XY - Mean	0.99
QuanTAV Morphology - Curvature Histogram - Bin 6	1.01
QuanTAV Morphology - Maximum Curvature per Vessel - Mean	1.05
QuanTAV Spatial Organization - Distance-Rotation - Kurtosis	1.07
QuanTAV Morphology - Skewness of Curvature Per Vessel - Mean	1.08
QuanTAV Spatial Organization - Distance-Rotation - Standard Deviation	1.24
QuanTAV Morphology - Deviation of Curvature Per Vessel - Standard Deviation	1.31

Supplementary Table 20. Cox proportional hazard univariable (UVA) and multivariable (MVA) analysis of recurrence free survival following NSCLC-TRI treatment, including QuanTAV risk score, QuanTAV risk groups, baseline clinical variables, and post-chemotherapy response and histolopathologic variables.

	Univariable		**Multivariable** Risk Score (Continuous)		**Multivariable** Risk Groups (Categorical)	
Variable	Hazard Ratio (95% CI)	p	Hazard Ratio (95% CI)	p	Hazard Ratio (95% CI)	p
QuanTAV Risk Score (increase of 1)	1.28 (1.01-1.62)	**0.039**	1.76 (1.16-2.67)	**0.008**	--	--
QuanTAV Risk Group (High vs. Low Risk)	3.77 (1.09-13.00)	**0.036**	--	--	31.91 (3.66-278.12)	**0.002**
Age (per year increase)	1.03 (0.98-1.07)	0.240	0.99 (0.92-1.07)	0.862	0.97 (0.90-1.05)	0.460
Sex (male vs. female)	1.16 (0.48-2.82)	0.738	0.46 (0.11-1.83)	0.270	0.52 (0.14-1.89)	0.320
Stage (IIIB vs IIIA)	1.17 (0.34-3.99)	0.807	0.79 (0.12-5.10)	0.803	0.20 (0.03-1.56)	0.126
Longest diameter (per mm increase)	1.00 (0.98-1.01)	0.684	1.02 (0.99-1.05)	0.145	1.05 (1.01-1.08)	**0.009**
Histology (Adenocarcinoma vs. SCC/other)	2.18 (0.79-6.02)	0.134	2.73 (0.54-13.89)	0.226	2.94 (0.57-15.05)	0.196
ECOG performance status (per grade increase)	0.86 (0.31-2.37)	0.767	1.78 (0.36-8.73)	0.477	1.01 (0.24-4.16)	0.990
Chemotherapy regimen (Cisplatin vs. Carboplatin)	0.39 (0.11-1.34)	0.135	0.19 (0.02-1.71)	0.140	0.11 (0.01-1.29)	0.079
Radiotherapy Induction Dose (per Gy increase)	0.98 (0.93-1.04)	0.537	1.11 (1.01-1.22)	**0.035**	1.14 (1.03-1.26)	**0.009**
Surgical procedure (pneumonectomy vs. lobectomy)	0.48 (0.16-1.44)	0.192	0.17 (0.03-1.05)	0.056	0.03 (0.00-0.30)	**0.003**
Presence of vascular invasion	3.56 (1.34-9.47)	**0.011**	5.31 (0.86-32.65)	0.071	6.45 (1.16-35.68)	**0.033**
Presence of lymphatic invasion	2.42 (0.98-6.00)	0.056	0.84 (0.17-4.07)	0.831	1.80 (0.42-7.75)	0.429

Supplementary Table 21. Pearson's correlation of top 5 most prognostic QuanTAV features and QuanTAV risk score with risk score derived from intra- and peri-tumoral texture features within the NSCLC-TRI cohort.

Feature	**Correlation Coefficient**	**p-value**
QuanTAV Morphology - Torsion Histogram - Bin 9	0.070	0.51
QuanTAV Spatial Organization - Distance-Rotation - Standard Deviation	-0.053	0.63
QuanTAV Spatial Organization - YZ - Skewness	-0.044	0.68
QuanTAV Morphology - Deviation of Curvature Per Vessel - Standard Deviation	0.0159	0.88
QuanTAV Morphology - Skewness of Curvature Per Vessel - Kurtosis	-0.408	**6.5E-05**
QuanTAV Prognostic Risk Score	0.229	**0.030**

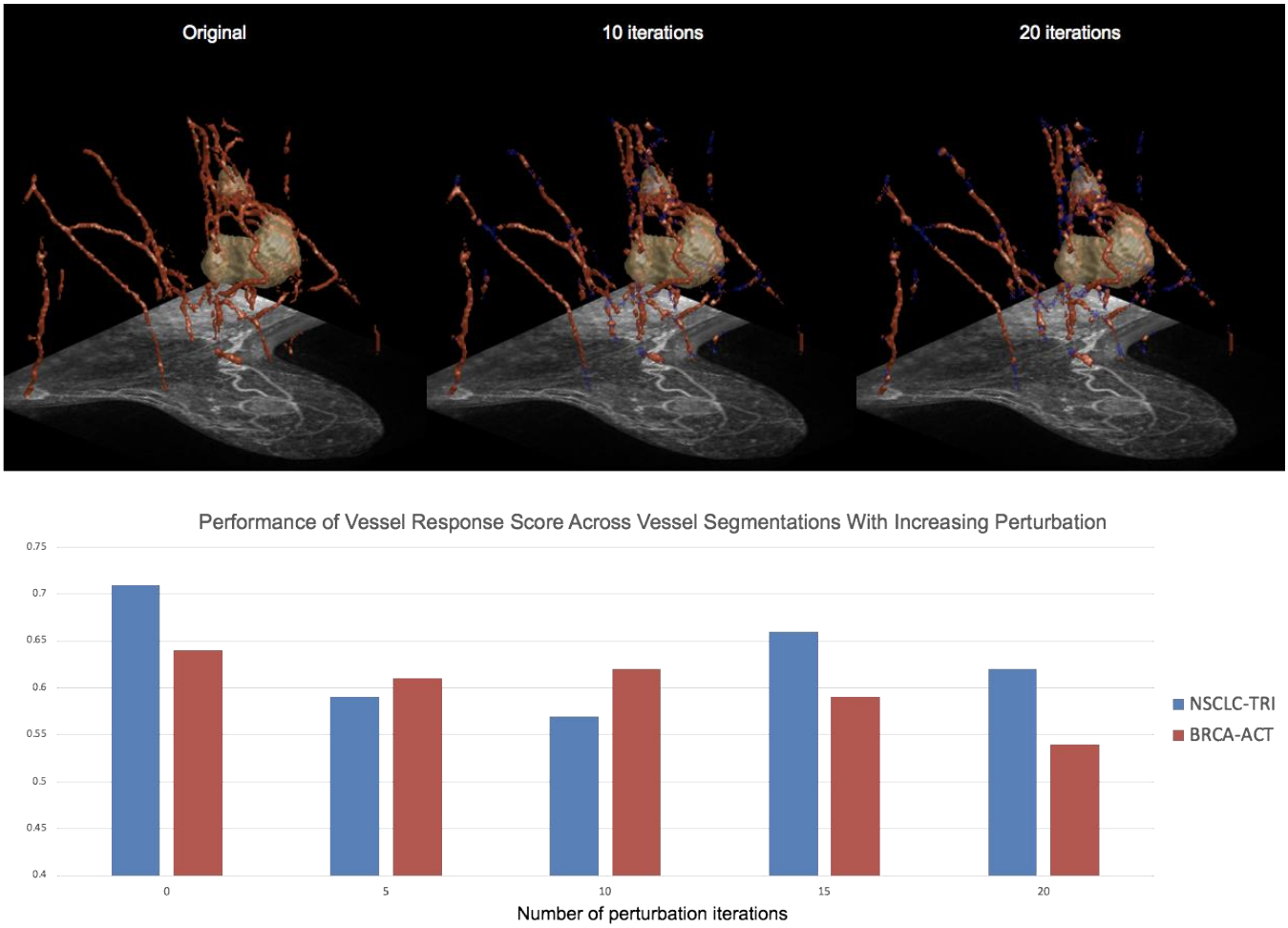

Supplementary Figure 4. Evaluating the robustness of QuanTAV-based response prediction to errors in vessel segmentation within a breast MRI (BRCA-ACT, n=144) and lung CT (NSCLC-TRI, n=46) testing set. Top: Vessel segmentations were randomly eroded and dilated at branchpoints and endpoints for increasing numbers of iterations. Vessel voxels in red were retained in the vasculature following perturbation, blue voxels indicate portions of the vasculature removed by perturbation. Bottom: QuanTAV response scores were re-computed using the vessel network at various levels of perturbation. Robustness of QuanTAV response score was assessed by computing the AUC of the ROC curves at each perturbation level (5, 10, 15, and 20 iterations of perturbation). When compared with the ROC curve of the QuanTAV response score computed with the original skeletons via Delong's test, no level of perturbation was found to produce a significant difference in AUC in either the NSCLC-TRI (p=0.12-0.65) or BRCA-ACT (p=0.11-0.30) cohorts.

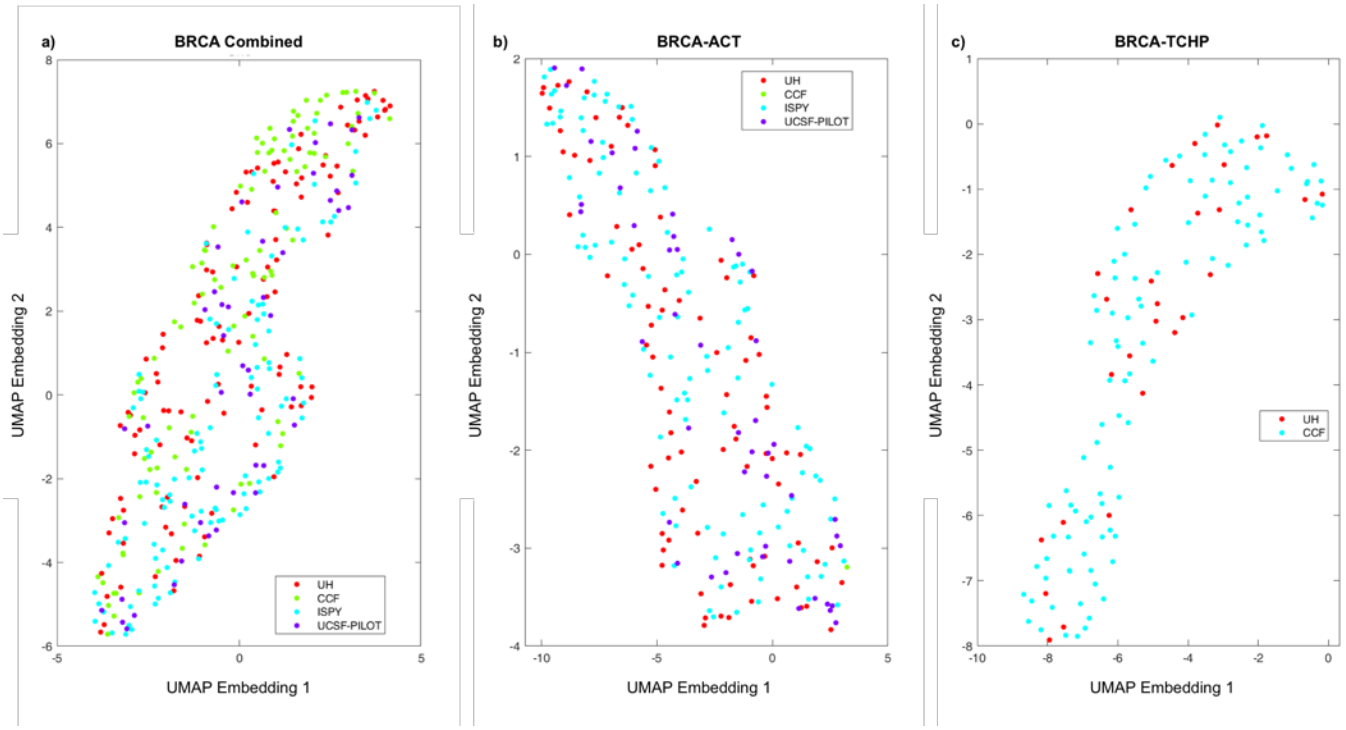

Supplementary Figure 5. UMAP projections of QuanTAV features for (a) all breast cancer patients, (b) the HER2-negative cohort receiving BRCA-ACT, (c) the HER2-positive cohort receiving BRCA-TCHP, shaded according to site. Some separation by site is observed across all patients (a), but this effect disappears when separated by HER2 status/treatment cohort (b&c). UH: University Hospitals, CCF: Cleveland Clinic Foundation, ISPY: ISPY1-TRIAL, UCSF-PILOT: University of California San Francisco ISPY1 pilot study.

Supplementary Methods – Implementation Details

Vessel Segmentation

The vesselness filtering utilized to extract the tumor vasculature involves a number of parameters to control the emphasis of vessel-like objects within an image. Supplementary Table 22 includes a description of each parameter and their settings for each modality. Settings were identical between modalities, aside from foreground threshold *C* which was altered on a per image basis for breast MRI scans, due to lack of consistent quantitative values between MRI scanners.[1]

Supplementary Table 22. Parameters for vesselness filtering of each imaging modality.

Parameter	Description	Lung CT value	Breast MRI value
α	Sensitivity parameter for metric that distinguishes between lines (vessel-like objects) and plate-like structures	0.5	0.5
β	Sensitivity parameter for metric that distinguishes between lines (vessel-like objects) and blob-like structures	0.5	0.5
C	Threshold for distinguishing background noise and vessel structure.	20	½ the maximum of the Hessian norm*
Scale	Parameter specifying expected radius of the detected vessels	1	1

*Due to the lack of absolute quantitative intensity values in MRI, *C* was set automatically on a per image basis proportional to the norm of its Hessian matrix. We chose a value of half the maximum of the Hessian norm, a value recommended for images with variable intensity ranges such as MR angiography by Frangi et al.[1]

QuanTAV Spatial Organization Features

QuanTAV organization features include several tunable parameters that were optimized to each imaging modality and cancer. A grid search was performed to optimize the radius from the tumor to include in spherical vessel projections and the size of the sliding window used to compute local vessel orientations. Vessel distances ranging from 5 to 20 mm from the tumor and sliding window sizes of [20, 35, 50, and 65] pixels were explored in the grid search. Step size for the moving window was fixed to 1/3 of the window size, and spherical coordinates were projected to images of size 400x400 pixels. For each pair of settings evaluated, features were extracted and used to train a classifier in 3-fold cross-validation within the training sets without feature selection. The configuration that maximized the minimum AUC of classifiers across all treatment groups for each modality was chosen as the optimal configuration for that cancer type. Thus, our search prioritized finding a set of QuanTAV organization features that performed well across all treatment contexts for a given imaging modality. Supplementary Figure 6 depicts the performance of QuanTAV organization features at each pair of distance and window settings. The optimal configuration of QuanTAV organization features for breast MRI was found to be a distance of 11 mm from the tumor and a window size of 35 pixels. For NSCLC on CT images, a distance of 7 mm from the tumor and window size of 20 pixels was found to be most effective.

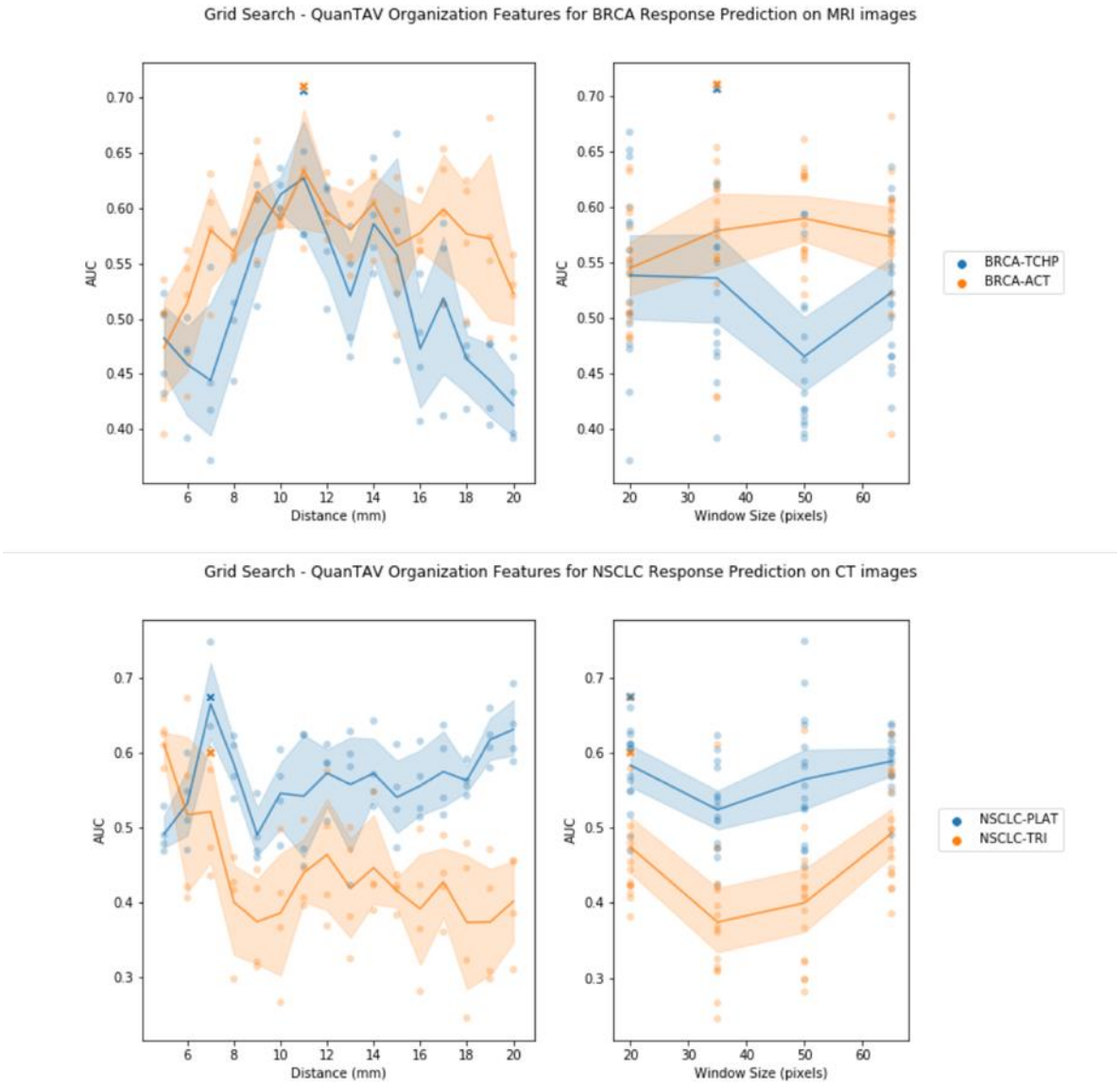

Supplementary Figure 6. Area under the receiver-operating curve (AUC) in grid searches to optimize QuanTAV Organization features for breast MRI (top), including the BRCA-ACT and BRCA-TCHP treatment groups and chest CT (bottom), including the NSCLC-PLAT and NSCLC-TRI treatment groups. QuanTAV Organization features were extracted at various combinations of inclusion radius and sliding window size settings within each training set and evaluated in cross-validation. For each imaging modality, the settings that maximized the performance of the worst-performing of the two treatment cohort models were chosen as the ideal configuration.

QuanTAV Predictive Response Score

A two-stage feature selection process was employed to choose a set of QuanTAV features to include in each QuanTAV predictive response score. First, feature selection was performed separately within the two feature groups (QuanTAV Morphology and QuanTAV Spatial Organization) to prune the size of the feature set. A second round of feature selection was then applied to this combined set of remaining QuanTAV Morphology and Spatial Organization features to identify a single best-performing feature set. In both stages, top features were chosen by Wilcoxon rank-sum test in cross-validation. These steps were repeated and re-evaluated with feature sets of sizes between one and six features. The optimal feature selection scheme and size was chosen based on the performance of a linear discriminant analysis (LDA) classifier within the training set in cross-validation.

QuanTAV Prognostic Risk Score

The QuanTAV feature set was first reduced to a set of uncorrelated features. The correlation between each pair of features was computed. For a set of correlated features, indicated by a Pearson correlation coefficient (r) with an absolute value greater than r_{min}, the feature with the greater p value in a two-feature Cox proportional hazards model was removed. From the set of retained, uncorrelated features, a Cox regression model was trained and optimized via 10-fold elastic net regularization with an elastic net mixing parameter of λ. The size of the feature set included in each model was determined by the number of features that minimized the deviance in cross-validation, with a minimum and maximum of 5 and 15 features. Values of λ and p were evaluated in a grid search and chosen based upon maximum performance across all cohorts during nested cross-validation in the training set, with chosen values corresponding to λ=0.01 and r_{min}=0.8. The coefficient values for the model were then applied to corresponding training and validation sets to derive patient risk scores. Risk score thresholds to stratify patients into high and low risk groups were also derived in the training as previously described[2]. For each prognostic risk score, a cutoff that best separated patients into high and low-risk groups was identified in the training set. Thresholds were first discarded that produced a group smaller than one-quarter of the training set or a log rank test p-value >0.05 were discarded. Among the set of thresholds with the maximum absolute difference in median survival time between groups, the final threshold was chosen by maximum hazard ratio. The derived risk score and risk groups were then applied to the training and testing sets. Models were trained using a modified version of the glmnet package[3] and evaluated using the MatSurv package for survival analysis in MATLAB.[4]

Supplementary Methods – Additional Experiments

QuanTAV association with texture-based risk assessment

Within the NSCLC-TRI cohort, a previously published[5] prognostic risk score for trimodality recipients composed of image texture features was assessed for correlations with prognostic QuanTAV features and risk score. The textural risk score consisted of 2 intra-tumoral features and 3 peri-tumoral features extracted within a 15 mm radius from the tumor. The top five most prognostic features of the QuanTAV signature were assessed for correlation with textural risk score in the full NSCLC-TRI cohort. The correlation with overall QuanTAV prognostic risk score was also assessed. In addition, a Cox model combining QuanTAV and texture risk scores was derived in the training set and applied to the testing set to evaluate their potential complementary values in risk assessment.

Effect of Segmentation Error on QuanTAV signatures.

To investigate the robustness of QuanTAV-based outcome predictions to errors in vessel segmentations, we evaluated the performance of QuanTAV response score at various reduced qualities of vessel segmentation. For each iteration, the set of all branchpoints and endpoints within the vessel skeleton were first identified. At each of these points, the vasculature was randomly perturbed with an equal chance to 1) erode the vessel locally, 2) dilate the vessel locally, or 3) make no change. Degraded vessel segmentations were saved after 5, 10, 15, and 20 iterations of perturbations (depicted in Supplementary Figure 4). Skeletons and QuanTAV features were then re-computed for each perturbed segmentation. The experiment was conducted on the testing sets from one breast (BRCA-ACT) and one lung (NSCLC-TRI) treatment group. QuanTAV response scores were then re-derived on the perturbed testing data and AUC was computed, which was then compared against perform of the original model via DeLong's test of paired ROC curves.[6]

Supplementary References

1. Frangi, A. F., Niessen, W. J., Vincken, K. L. & Viergever, M. A. Multiscale vessel enhancement filtering. in *Medical Image Computing and Computer-Assisted Intervention — MICCAI'98* 130–137 (Springer, Berlin, Heidelberg, 1998). doi:10.1007/BFb0056195.

2. Bhargava, H. K. *et al.* Computationally Derived Image Signature of Stromal Morphology Is Prognostic of Prostate Cancer Recurrence Following Prostatectomy in African American Patients. *Clin. Cancer Res.* **26**, 1915–1923 (2020).

3. Glmnet in Matlab. http://web.stanford.edu/~hastie/glmnet_matlab/.

4. MatSurv. https://www.mathworks.com/matlabcentral/fileexchange/64582-matsurv.

5. Khorrami, M. *et al.* Predicting pathologic response to neoadjuvant chemoradiation in resectable stage III non-small cell lung cancer patients using computed tomography radiomic features. *Lung Cancer* **135**, 1–9 (2019).

6. DeLong, E. R., DeLong, D. M. & Clarke-Pearson, D. L. Comparing the areas under two or more correlated receiver operating characteristic curves: a nonparametric approach. *Biometrics* **44**, 837–845 (1988).